Thermodynamics of CFTR Channel Gating: A Spreading Conformational Change Initiates an Irreversible Gating Cycle

László Csanády,[1] Angus C. Nairn,[2] and David C. Gadsby[3]

[1]Department of Medical Biochemistry, Semmelweis University, 1088 Budapest, Hungary
[2]Laboratory of Molecular and Cellular Neuroscience and [3]Laboratory of Cardiac/Membrane Physiology, Rockefeller University, New York, NY 10021

CFTR is the only ABC (ATP-binding cassette) ATPase known to be an ion channel. Studies of CFTR channel function, feasible with single-molecule resolution, therefore provide a unique glimpse of ABC transporter mechanism. CFTR channel opening and closing (after regulatory-domain phosphorylation) follows an irreversible cycle, driven by ATP binding/hydrolysis at the nucleotide-binding domains (NBD1, NBD2). Recent work suggests that formation of an NBD1/NBD2 dimer drives channel opening, and disruption of the dimer after ATP hydrolysis drives closure, but how NBD events are translated into gate movements is unclear. To elucidate conformational properties of channels on their way to opening or closing, we performed non-equilibrium thermodynamic analysis. Human CFTR channel currents were recorded at temperatures from 15 to 35°C in inside-out patches excised from *Xenopus* oocytes. Activation enthalpies ($\Delta H^{\ddagger}$) were determined from Eyring plots. $\Delta H^{\ddagger}$ was 117 ± 6 and 69 ± 4 kJ/mol, respectively, for opening and closure of partially phosphorylated, and 96 ± 6 and 73 ± 5 kJ/mol for opening and closure of highly phosphorylated wild-type (WT) channels. $\Delta H^{\ddagger}$ for reversal of the channel opening step, estimated from closure of ATP hydrolysis–deficient NBD2 mutant K1250R and K1250A channels, and from unlocking of WT channels locked open with ATP+AMPPNP, was 43 ± 2, 39 ± 4, and 37 ± 6 kJ/mol, respectively. Calculated upper estimates of activation free energies yielded minimum estimates of activation entropies ($\Delta S^{\ddagger}$), allowing reconstruction of the thermodynamic profile of gating, which was qualitatively similar for partially and highly phosphorylated CFTR. $\Delta S^{\ddagger}$ appears large for opening but small for normal closure. The large $\Delta H^{\ddagger}$ and $\Delta S^{\ddagger}$ ($T\Delta S^{\ddagger} \geq 41$ kJ/mol) for opening suggest that the transition state is a strained channel molecule in which the NBDs have already dimerized, while the pore is still closed. The small $\Delta S^{\ddagger}$ for normal closure is appropriate for cleavage of a single bond (ATP's beta-gamma phosphate bond), and suggests that this transition state does not require large-scale protein motion and hence precedes rehydration (disruption) of the dimer interface.

The Journal of General Physiology

INTRODUCTION

Cystic fibrosis is caused by mutations in the gene that encodes CFTR (Riordan et al., 1989), the only known ion channel in the ATP-binding cassette (ABC) superfamily of transport proteins. CFTR's two homologous halves are linked via a cytoplasmic regulatory (R) domain not found in other ABC proteins; each half comprises a transmembrane domain, which contributes to the ion pore, attached to a cytoplasmic nucleotide-binding domain (NBD1 or NBD2) (Riordan et al., 1989). CFTR channel gating is driven by ATP binding and hydrolysis at the NBDs (Anderson et al., 1991), but requires prior phosphorylation of the R domain by cyclic AMP–dependent protein kinase (PKA; Tabcharani et al., 1991). Two gating modes have been reported: CFTR channel open bursts are long in the presence of PKA but shorten upon PKA removal, presumably reflecting rapid partial dephosphorylation (Hwang et al., 1994; Zeltwanger et al., 1999; Csanády et al., 2000). The mechanisms by which ATP and PKA together regulate CFTR channel gating are complex (e.g., Gadsby and Nairn, 1999; Gadsby et al., 2006) and controversial (e.g., Aleksandrov et al., 2000; Vergani et al., 2003; Bompadre et al., 2005).

Early observations that phosphorylated wild-type (WT) CFTR channels were opened readily by hydrolyzable, but not by nonhydrolyzable, ATP analogues (Anderson et al., 1991; Nagel et al., 1992; Hwang et al., 1994), and that channel closure was markedly delayed when orthovanadate (Baukrowitz et al., 1994; Gunderson and Kopito, 1994) or the nonhydrolyzable ATP analogue AMPPNP (Hwang et al., 1994; Gunderson and Kopito, 1994; Carson et al., 1995) was included with ATP, led to the interpretation that both opening and closing might require ATP hydrolysis (for review see Gadsby and Nairn, 1999); extreme slowing of both opening and closing of CFTR channels upon removal of free Mg^{2+} supported that proposal (Dousmanis et al., 2002). However, mutations in conserved sequences (Walker A or B; Walker et al., 1982) expected to impair ATP hydrolysis little influenced CFTR gating (at saturating [ATP]) when introduced into NBD1, but greatly prolonged open bursts when made in NBD2 (Carson et al., 1995; Gunderson

Correspondence to László Csanády: csanady@puskin.sote.hu; or David C. Gadsby: gadsby@rockefeller.edu

The online version of this article contains supplemental material.

Abbreviations used in this paper: ABC, ATP-binding cassette; NBD, nucleotide-binding domain; R, regulatory; WT, wild type.

and Kopito, 1995; Zeltwanger et al., 1999; Powe et al., 2002; Vergani et al., 2003). Also, millimolar concentrations of nonhydrolyzable ATP analogues were found to support CFTR channel opening (Aleksandrov et al., 2000), albeit far less effectively than ATP (Vergani et al., 2003). In addition, although ATPase measurements confirmed that CFTR hydrolyzes ATP (Li et al., 1996), photolabeling studies found ATP hydrolysis only at the catalytic site incorporating NBD2 Walker sequences (Aleksandrov et al., 2002), not that with NBD1 Walker residues (Basso et al., 2003).

Mechanistic interpretation of these results was aided by the finding that prokaryotic NBDs form head-to-tail dimers, X-ray crystal structures of which revealed two interfacial composite catalytic sites each with a bound ATP; each site comprised the Walker A and B residues of one NBD and the conserved ABC signature (LSGGQ-like) sequence of the other (e.g., Hopfner et al., 2000; Smith et al., 2002). Because a Walker-B Glu mutation in CFTR's NBD2, corresponding to a hydrolysis-impairing mutation that promoted stable dimerization of prokaryotic NBDs by ATP (Smith et al., 2002), yielded channels with greatly stabilized open bursts, lasting minutes (Vergani et al., 2003, 2005), the open-channel state was proposed to be a CFTR conformation with an intramolecular NBD1–NBD2 dimer. As mutations impairing ATP binding at either NBD reduced the apparent affinity with which ATP elicits channel opening, it was suggested (Vergani et al., 2003) that formation of the NBD1–NBD2 dimer, and hence of the open channel state, is preceded by ATP binding to both NBDs. On the other hand, disruption of that dimer, and hence channel closure, was suggested to be normally preceded by hydrolysis only of the ATP bound at the composite "NBD2" catalytic site (comprising NBD2 Walker motifs and NBD1 signature sequence).

Analysis of temperature dependence of reaction rates can illuminate molecular mechanisms by dissecting enthalpic and entropic contributions to overall activation free energies of molecules during transitions from one stable conformation to another. Ion channel gating is well suited to such analyses because in patch-clamp recordings the timing of individual conformational transitions of single molecules can be conveniently observed (Hamill et al., 1981) and quantified (e.g., Colquhoun and Sigworth, 1995; Qin et al., 1996). So far, however, the limited analyses of temperature dependence of CFTR channel gating have yielded differing conclusions (Aleksandrov and Riordan, 1998; Mathews et al., 1998b), in part perhaps because gating of CFTR is not a thermodynamic equilibrium process, a fact that rules out the conventional analytical approach used in one of the studies (Aleksandrov and Riordan, 1998).

Here we examine the temperature dependence of opening and closing of WT CFTR channels in both the long-burst (in the presence of PKA), and the shorter-burst (after PKA removal), gating mode. By also studying the temperature dependence of the extremely slow closure of the channel under conditions in which normal rapid closure by a mechanism proposed to involve ATP hydrolysis was prevented, we were able to outline a partial energetic profile of CFTR's irreversible gating cycle. Our results reveal the activation enthalpy for channel closure to be large, and that for opening to be even larger. Phosphorylation extent does not affect the activation enthalpy for closure, suggesting that it modulates the rate, but not the molecular mechanism, of channel closing. Our analysis identifies a conformation of CFTR during channel opening in which its gating machinery (i.e., the NBDs) has already adopted its open-state configuration, believed to require formation of an NBD1–NBD2 dimer (Vergani et al., 2005), while the pore itself is still closed. These results indicate that a spreading conformational change beginning at the cytoplasmic NBDs and propagating to the transmembrane domains precedes CFTR channel opening. Our analysis further suggests that closure of the channel pore is rate limited by a step that does not involve large-scale protein motion, consistent with hydrolysis of a single chemical bond, such as that between the β and γ phosphates of ATP bound at the composite NBD2 catalytic site. These data offer new insight into the mechanism by which the NBD ATPase cycle is coupled to conformational changes of the transmembrane domains in this representative ABC protein.

MATERIALS AND METHODS

Molecular Biology

pGEMHE-WT was constructed as previously described (Chan et al., 2000), and the K1250R and K1250A mutations introduced using QuikChange (Stratagene) as previously described (Vergani et al., 2003, 2005).

Isolation and Injection of *Xenopus* Oocytes

Xenopus laevis oocytes were treated with collagenase, isolated, and injected as previously described (Chan et al., 2000). Oocytes were injected with 0.1–10 ng CFTR cRNA to obtain expression levels suitable for single-channel or macroscopic current recordings, respectively, and stored at 18°C in a Ringer's solution supplemented with 1.8 mM $CaCl_2$ for 2–3 d before recording.

Excised-patch Recording

Patch pipettes were pulled from borosilicate glass and fire polished to tip resistances of ~2 MΩ for recording macroscopic currents or ~6 MΩ for single-channel recordings. Pipette solution contained (in mM) 136 NMDG-Cl, 2 $MgCl_2$, 5 HEPES, pH 7.4 with NMDG. Bath solution contained (in mM) 134 NMDG-Cl, 2 $MgCl_2$, 5 HEPES, 0.5 EGTA, pH 7.1 with NMDG. Seal resistances were typically >100 GΩ, and patches were excised into an inside-out configuration. 2 mM MgATP (Sigma-Aldrich) was added from a 400 mM aqueous stock solution (pH 7.1 with NMDG). 1 mM Li_4-AMPPNP (Sigma-Aldrich) was added from a 400 mM aqueous stock solution, supplemented with equimolar $MgCl_2$. 300 nM catalytic subunit of PKA was added to activate CFTR channels. This high specific activity PKA (>95% pure) was extracted from bovine

heart (Kaczmarek et al., 1980) and stored in a 150 mM potassium-phosphate buffer (pH 7.0) containing 1 mM EDTA and 15 mM β-mercaptoethanol. At the dilution used for our recordings, the final concentration of phosphate was 1.8 mM, a concentration that little affects CFTR channel gating (Carson et al., 1994). Inward unitary and macroscopic currents were recorded at a membrane potential of −80 mV (pipette holding potential = +80 mV), digitized at 1 kHz, and recorded to disk using on-line Gaussian filtering at 50 Hz (pCLAMP 8; Axon Instruments, Inc.). Large macroscopic currents from thousands of channels were occasionally recorded at −40 or −20 mV, which did not influence the results of our analysis, as CFTR gating is largely voltage independent (see Fig. S2, available at http://www.jgp.org/cgi/content/full/jgp.200609558/DC1; also compare Cai et al., 2003).

Temperature Control

A custom-made flow chamber accommodated seven flow lines arranged concentrically around a small (∼0.5-mm diameter) thermistor (TH-30; Dagan Corporation). After excision, patches were transferred into this flow chamber in immediate vicinity (∼2 mm) of the thermistor, which therefore faithfully measured the temperature of the solution bathing the patch (see temperature traces in Fig. 1 B, Fig. 3 A, Fig. 4 A, and Fig. 5 A). The temperature of four of the flow lines was held at the desired test temperature (e.g., 15°C, 20°C, 31°C, or 35°C) using a TC-10 temperature contoller (Dagan), while the remaining lines contained solutions at 25°C. Only one flow line was active at any time, and changes in temperature and composition of the solution superfusing the patch were effected by switching the active flow line using electronic valves. Although the composition of the bath could be exchanged with a time constant of ∼100 ms (judged from the rate of decay of endogenous Ca^{2+}-activated Cl^- current; Csanády et al., 2000, 2005), temperature could be changed only much more slowly due to the heat capacity of the flow chamber; a 10°C temperature jump typically required 20–30 s. Nevertheless, this arrangement allowed recording of channel activity from the same patch exposed to different temperatures in a bracketed fashion, together with faithful recording of the temperature time course.

Steady-state Kinetic Analysis

Current records from patches with few channels, in which individual channel transitions could be clearly resolved, were baseline subtracted to remove slow drifts, e.g., due to temperature-dependent changes in seal current. Baseline-subtracted currents were idealized using half-amplitude threshold crossing, with imposition of a fixed dead time of 6.5 ms (Csanády, 2000a), and the resulting events lists subjected to kinetic analysis as previously described (Csanády et al., 2000). In brief, ATP-dependent slow gating was pooled into a simple closed–open scheme and rapid flickery closures modeled as pore-blockage events. Rate constants (r_{CO}, r_{OC}, r_{OB}, r_{BO}) of the resulting Closed–Open–Blocked scheme were extracted by a simultaneous maximum likelihood fit to the dwell-time histograms of all conductance levels, using an algorithm that includes a correction for the filter dead time (Csanády, 2000a). Mean closed interburst (τ_{ib}) and open burst (τ_b) durations were then calculated as $\tau_{ib} = 1/r_{CO}$, and $\tau_b = (1/r_{OC})(1 + r_{OB}/r_{BO})$. Rates of opening to a burst, and closing from a burst, are defined as $1/\tau_{ib}$ and $1/\tau_b$, respectively.

The number of active channels in the patch (N) was assumed to equal the maximum number of simultaneously open channels (N') seen in any record. Correct estimation of opening rates, unlike that of closing rates, depends heavily on correct estimation of N. To eliminate ambiguities arising from uncertainties in channel number, we studied only relative changes in kinetic rates brought about by sudden changes in temperature. Thus, we normalized the opening and closing rate extracted from segments of record at any test temperature to the average of the corresponding rates in bracketing segments of record, from the same channels in the same patch, at our control temperature of 25°C (see Fig. 1). This procedure also corrected both for gradual, temperature-independent, changes in gating parameters occurring in a given patch during an experiment (channel rundown), as well as for heterogeneity in channel kinetics between different patches.

Analysis of Macroscopic Current Relaxations

Macroscopic current decay time courses were fit by single or double exponential functions using pCLAMP 8 software (Axon Instruments, Inc.).

Thermodynamic Analysis

Upper limits for activation free energies ($\Delta G^{\ddagger}$) for single-channel opening and closing transitions were obtained using transition state theory (e.g., Fersht, 1999). According to this formalism, a chemical reaction (in the present case a transition, in either direction, between the relatively stable closed and open-burst conformations of the channel protein, both kinetically zero-order reactions at saturating, 2 mM, [ATP]) proceeds through an unstable high free energy transition state; the activation free energy, $\Delta G^{\ddagger}$, is the free energy of that transition state relative to the ground state. A transition rate k can be calculated as

$$k = \kappa \cdot A^{*} \cdot e^{-\frac{\Delta G^{\ddagger}}{RT}},$$

where κ ($0 \le \kappa \le 1$; the "transmission coefficient") is the fraction of formed transition state complexes that proceeds toward the product. One estimate of the prefactor A^* was given by Eyring in the form of $k_B T/h$, where k_B is Boltzmann's constant, T is temperature in °K, h is Planck's constant ($k_B T/h \approx 6 \times 10^{12}$ s^{-1} at 25°C). Although originally developed for reactions in the gas phase, transition state theory has been successfully applied to rates of reactions in solution, such as GTP hydrolysis by the small GTPase p21-ras (Schweins and Warshel, 1996) or protein–protein dimer formation (Frisch et al., 2001), by using Eyring's prefactor and assuming $\kappa = 1$. On the other hand, experiments under conditions in which it was assumed that $\Delta G^{\ddagger} \approx 0$ yielded maximal reaction rates on the order of 10^6 s^{-1} for protein folding (Hagen et al., 1996) and, perhaps more relevant, also for the pore-opening transition of the liganded nicotinic acetylcholine receptor (Chakrapani and Auerbach, 2005), suggesting that for these reactions the prefactor A^* might be much smaller than $k_B T/h$ (because, at least for the latter reaction, κ is not vanishingly small; Zhou et al., 2005). This uncertainty in A^* and κ necessarily clouds absolute $\Delta G^{\ddagger}$ values obtained by this method for reactions that involve large protein conformational changes. Nevertheless, using Eyring's prefactor and setting $\kappa = 1$ allows determination of a safe maximum estimate for $\Delta G^{\ddagger}$. Thus, $\Delta G^{\ddagger} \le RT\ln(k_B T/(kh))$ or $\Delta G^{\ddagger}_{max} = RT\ln(k_B T/(kh))$.

Activation enthalpy ($\Delta H^{\ddagger}$) is obtained by substituting $\Delta G^{\ddagger} = \Delta H^{\ddagger} - T\Delta S^{\ddagger}$, so that,

$$\ln\left(\frac{k}{T}\right) = \ln\frac{k_B \kappa}{h} + \frac{\Delta S^{\ddagger}}{R} - \frac{\Delta H^{\ddagger}}{R} \cdot \frac{1}{T},$$

and $\Delta H^{\ddagger}$ is the slope of a plot of $\ln(k/T)$ vs. $1/T$ (Eyring plot) multiplied by $(-R)$. As that slope does not depend on κ, the $\Delta H^{\ddagger}$ estimate is not subject to the uncertainty discussed for $\Delta G^{\ddagger}$. From $\Delta H^{\ddagger}$ and $\Delta G^{\ddagger}_{max}$, a lower limit for $\Delta S^{\ddagger}$ can be set: $T\Delta S^{\ddagger} \ge \Delta H^{\ddagger} - \Delta G^{\ddagger}_{max}$, or $T\Delta S^{\ddagger}_{min} = \Delta H^{\ddagger} - \Delta G^{\ddagger}_{max}$.

Statistics

Symbols and error bars in figures report mean ± SEM.

Online Supplemental Material

This paper contains online supplemental material available at http://www.jgp.org/cgi/content/full/jgp.200609558/DC1. Fig. S1

shows simultaneous unitary current and temperature records illustrating temperature dependence of gating of highly phosphorylated WT CFTR channels at −80 mV. Figs. S2–S4 show parallel macroscopic current and temperature records illustrating temperature dependence of closure of partially phosphorylated K1250R and K1250A, and of AMPPNP-locked WT, CFTR, respectively, recorded at −80 to −20 mV between 25°C and 31°C. Fig. S5 demonstrates that exposure to millimolar levels of the hydrolysis products ADP+P_i does not cause opening of prephosphorylated WT CFTR channels. Fig. S6 shows the predicted energetic profile of CFTR gating obtained using K1250A, not K1250R (as in Fig. 6), as a model for nonhydrolytic channel closure.

RESULTS

Open probability (P_o) of CFTR channels increases with extent of PKA-mediated phosphorylation (Chang et al., 1993; Mathews et al., 1998a; Csanády et al., 2005). P_o immediately declines by ∼50% on removal of 300 nM PKA catalytic subunit from MgATP-bathed patches excised from *Xenopus* oocytes expressing WT human CFTR (e.g., Fig. 1 A); this correlates with a greater than twofold reduction in open-burst duration, from ∼700 to <300 ms (Csanády et al., 2000; Fig. 1 A, insets), presumably due to rapid dephosphorylation of some R-domain serine(s) by membrane-bound phosphatases. This rapid partial dephosphorylation is not prevented by inhibition of phosphatases 1 and 2A with microcystin, and of phosphatase 2B by the absence of Ca^{2+} (Csanády, 2000b). It is followed by a much slower decline of average current over a time course of many minutes (e.g., Csanády et al., 2000; compare Fig. 1 and Fig. S4), during which the pattern of CFTR channel gating remains relatively well defined (e.g., Chan et al., 2000; Csanády et al., 2000, 2005; Vergani et al., 2003, 2005). An experimental design incorporating strict bracketing (see Materials and methods) can therefore largely compensate for this slow unidirectional change in gating parameters in the partially dephosphorylated state, reached within a few seconds of PKA removal. On the other hand, in the continued presence of 300 nM PKA, a near-saturating concentration (Csanády et al., 2005), a large fraction of the ∼10 phosphorylatable serines in a CFTR channel's R-domain will remain phosphorylated at any moment. Although dephosphorylation/rephosphorylation events no doubt occur under those conditions, they are expected to have little effect on gating, as the functional impact of a single phosphoserine is small (Cheng et al., 1991; Chang et al., 1993). We could therefore examine the gating behavior of CFTR channels under two distinct, well-characterized conditions, highly phosphorylated in the presence of PKA and partially dephosphorylated shortly after PKA withdrawal.

Temperature Dependence of Gating of Partially Dephosphorylated CFTR Channels

We first tested the temperature dependence of gating of partially dephosphorylated CFTR channels (Fig. 1) at saturating, 2 mM, [MgATP] (e.g., Csanády et al., 2000; Vergani et al., 2003) after PKA withdrawal, by recording at 25°C (Fig. 1 A, blue), and at some test value (e.g., 31°C in Fig. 1 A, red), in a bracketed fashion. Both opening and closing rates were increased by warming (Fig. 1 A, insets), but the speeding of opening was greater, as overall P_o was larger at more elevated temperatures (Fig. 1 A). Linear fits to Eyring plots (Fig. 1 C) of normalized opening rates (red symbols) and closing rates (black symbols) at 15, 25, 31, and 35°C yielded estimates of $\Delta H^{\ddagger}$ for the opening and closing transitions that were both large, but $\Delta H^{\ddagger}$ for opening (117 ± 6 kJ/mol) was much larger than for closing (69 ± 4 kJ/mol).

Temperature Dependence of Gating of CFTR Channels in the Presence of PKA

The longer open burst durations, and enhanced susceptibility to becoming locked open by mixtures of ATP and AMPPNP, of highly phosphorylated CFTR channels (Hwang et al., 1994; Mathews et al., 1998a,b) led to the proposal that their gating cycles might differ qualitatively from those of partially phosphorylated channels, with ATP hydrolysis limiting closure of only highly phosphorylated CFTR (for review see Gadsby and Nairn, 1999). Because different temperature dependence might betray different molecular mechanisms, we repeated experiments like those of Fig. 1 but in the continued presence of 300 nM PKA to sustain high levels of phosphorylation (Fig. S1, available at http://www.jgp.org/cgi/content/full/jgp.200609558/DC1). Once again, despite longer mean burst durations at lower temperatures, average P_o was smaller, indicating that a temperature drop compromised opening even more than closing. Accordingly, as found for partially phosphorylated channels (Fig. 1 C), Eyring plots for highly phosphorylated channels (Fig. 2) revealed steep temperature dependence for both opening rates (red symbols) and closing rates (black symbols), and $\Delta H^{\ddagger}$ was again larger for the opening transition (96 ± 6 kJ/mol) than for closure (73 ± 5 kJ/mol).

Temperature Dependence of Closing Rate of Hydrolysis-deficient Mutant K1250R and K1250A CFTR Channels

To estimate $\Delta H^{\ddagger}$ for channel closing when the normal route for channel closure via ATP hydrolysis was unavailable, we studied the temperature dependence of the closing rate of two channel constructs in which the composite NBD2 site was made catalytically inactive by mutation of the conserved NBD2 Walker A lysine, K1250. The mutation K1250A has been shown to abolish ATPase activity of purified CFTR (Ramjeesingh et al., 1999). In another ABC ATPase, P-glycoprotein, the Lys-to-Arg mutation of either Walker A lysine abolishes ATP hydrolysis (Lerner-Marmarosh et al., 1999), and in CFTR, the K1250R mutation prolongs open

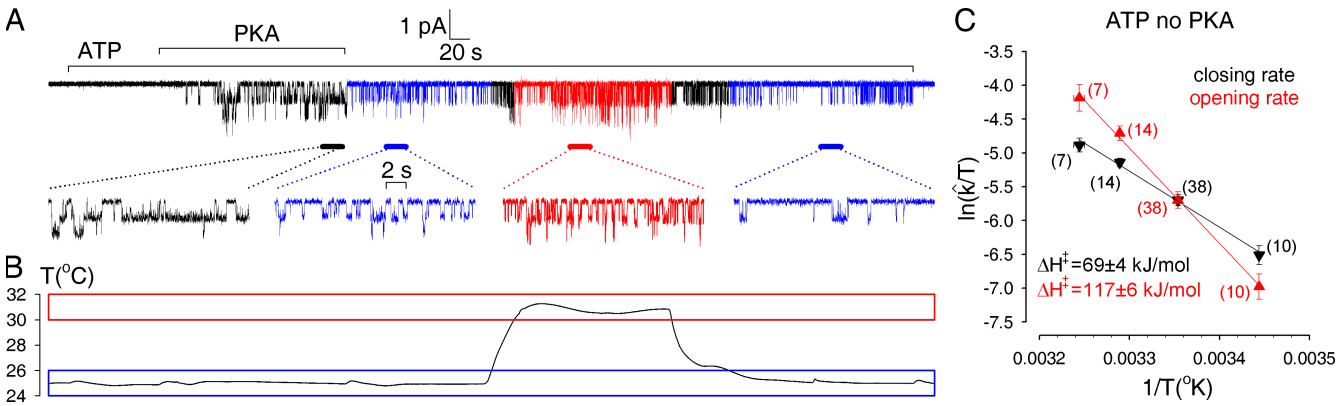

Figure 1. Temperature dependence of gating of partially phosphorylated WT CFTR. (A) Baseline-subtracted current trace of approximately three CFTR channels at −80 mV in 2 mM MgATP (bar, ATP) at 25°C (blue segments) and 31°C (red segment) after activation by 300 nM PKA (bar, PKA). Insets show expanded traces. (B) Temperature near the patch during current recordings in A; boxes identify the analyzed segments of experiment, i.e., segments with temperature 25 ± 1°C (blue box) or 31 ± 1°C (red box). (C) Eyring plot of opening (red symbols and line) and closing (black symbols and line) rates of partially phosphorylated WT CFTR in 2 mM MgATP at 15°C, 31°C, and 35°C, normalized ($\hat{k}$) to their average values in bracketing control segments at 25°C; straight lines were fitted to the plots to obtain $\Delta H^{\ddagger}$ values shown.

burst durations by >20-fold (compare Vergani et al., 2005), consistent with abolished, or greatly diminished, ATP hydrolysis. Closure of K1250R or of K1250A mutant CFTR channels is too slow to allow kinetic analysis of individual gating events and so it was assayed as current decay after sudden removal of ATP. Because opening is negligible at 0 [ATP], the time course of current loss gives the time constant of channel closing.

Prephosphorylated K1250R CFTR channels in macropatches were repeatedly opened by brief exposures to 2 mM MgATP at temperatures alternating between 25°C and ∼15°C (Fig. 3 A), or 25°C and ∼31°C (Fig. S2). Current decay after each ATP removal was fitted with a single exponential (Fig. 3 A, smooth lines) and channel closing rate was obtained as the reciprocal of that time constant. The Eyring plot of the normalized closing rates (Fig. 3 B) yielded a $\Delta H^{\ddagger}$ for nonhydrolytic closure of 43 ± 2 kJ/mol, which is substantially smaller than the value we found for normal closure of WT channels (Fig. 1 C).

Because the K1250A mutation greatly diminishes the affinity for ATP binding (Vergani et al., 2003), 10 mM MgATP was used to repeatedly activate macroscopic K1250A currents at temperatures alternating between 25°C and either ∼15°C (Fig. 4 A) or ∼31°C (Fig. S3). The Eyring plot (Fig. 4 B) of the normalized closing rates obtained from single exponential fits (Fig. 4 A, smooth lines) to the decaying currents after ATP removal yielded a $\Delta H^{\ddagger}$ for nonhydrolytic closure of 39 ± 4 kJ/mol, similar to that obtained for K1250R channels (Fig. 3 B).

Interestingly, whereas open burst duration of WT channels was greater than twofold longer in the presence of PKA than shortly after its withdrawal, the average closing time constant of K1250R at 25°C, equivalent to its mean open burst duration, was only slightly longer (Fig. 3 A; Fig. S2) upon removal of PKA+ATP (7.3 ± 0.8 s, $n = 12$) than upon removal of just ATP (5.7 ± 0.4 s, $n = 30$). But, because the fall in P_o that signals partial dephosphorylation of WT channels upon PKA removal occurs so rapidly (i.e., in 2–3 s; Csanády et al., 2000), the phosphorylation status of K1250R channels after removal of ATP+PKA, during their gradual closure, which takes tens of seconds (compare Fig. 3 A, current segments fitted by magenta lines), is uncertain. For K1250A channels, the closing time constant after simultaneous removal of ATP and PKA was rarely assessed ($\tau = 38 \pm 4$ s, $n = 3$), and is not easily compared with that after removal of just ATP ($\tau = 25 \pm 2$ s, $n = 29$), as the latter usually progressively shortened during an experiment ($\tau = 29 \pm 3$ s, $n = 18$, for the first decay from each

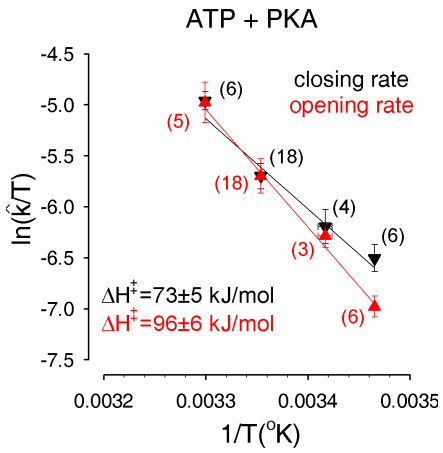

Figure 2. Temperature dependence of gating of highly phosphorylated WT CFTR. Eyring plot of normalized opening (red symbols) and closing (black symbols) rates ($\hat{k}$) of highly phosphorylated WT CFTR channels in 2 mM MgATP plus 300 nM PKA; linear fits yielded $\Delta H^{\ddagger}$ values shown.

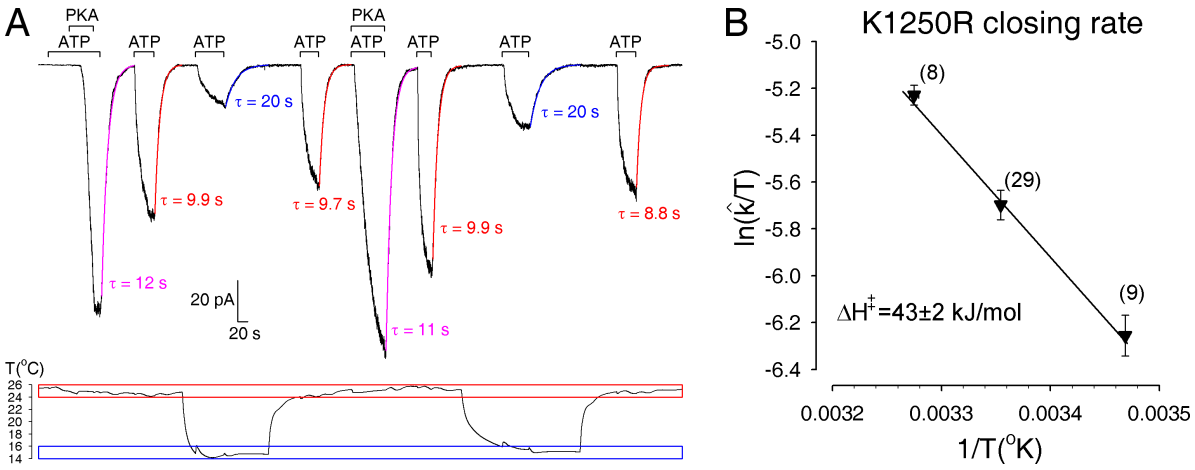

Figure 3. Temperature dependence of gating of partially phosphorylated K1250R CFTR. (A) Macroscopic current trace (top) from ~2,000 K1250R CFTR channels at −20 mV, with simultaneously recorded temperature (bottom). Prephosphorylated channels were repeatedly opened by brief exposures to 2 mM MgATP, while bath temperature was toggled between 25°C (red box) and 15°C (blue box). Single exponentials (colored smooth lines) fitted to all current decay time courses at 25°C (red curves) and 15°C (blue curves) yielded time constants (τ) shown. PKA was reapplied after the first bracketed experiment to recover channel activity lost due to slow dephosphorylation; note minimal influence on decay time constants of the presence of PKA during channel activation (magenta fit lines). (B) Eyring plot of normalized closing rates ($\hat{k}$) of K1250R CFTR channels upon ATP removal, fitted by a straight line to obtain $\Delta H^{\ddagger}$ value shown; closing rates, obtained as $1/\tau$ from single-exponential fits, as in A, were normalized to their average values in bracketing control segments at 25°C.

experiment). These technical difficulties prevent us from addressing the influence of phosphorylation on $\Delta H^{\ddagger}$ for nonhydrolytic closure.

Temperature Dependence of Closing Rate of WT CFTR Channels Locked Open by the Nonhydrolyzable ATP Analogue AMPPNP

As a third, independent, way to estimate $\Delta H^{\ddagger}$ for nonhydrolytic closure, we measured the temperature dependence of the closing rate of prephosphorylated WT CFTR channels that had been locked in the open-burst state by simultaneous exposure to ATP (1 mM) plus AMPPNP (0.1 mM; Fig. 5 A).

On removal of ATP+AMPPNP, a large fraction of the current decayed rapidly, with a time constant of <1 s, just as after removal of 2 mM ATP alone, but a smaller-amplitude slower component was invariably present, reflecting a small fraction of locked-open channels

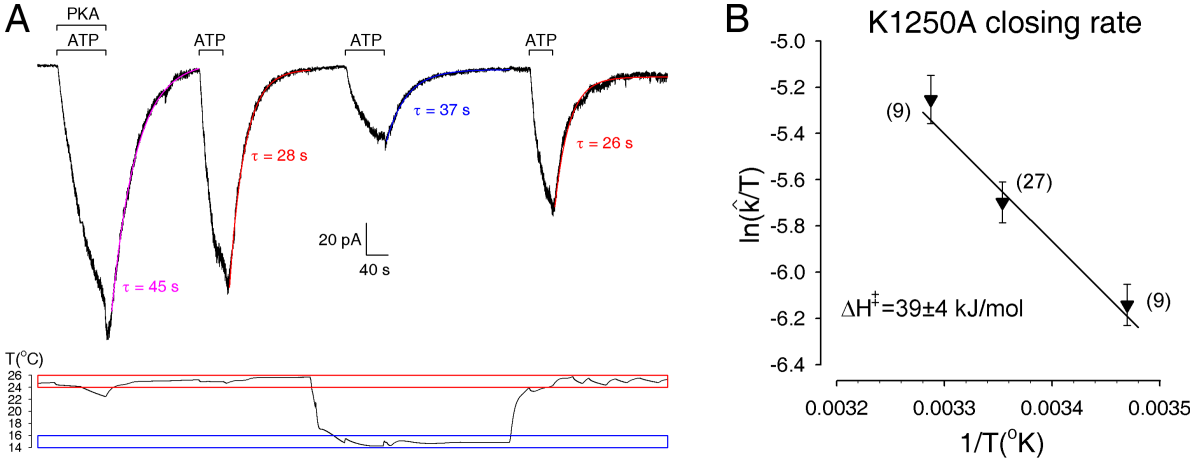

Figure 4. Temperature dependence of gating of partially phosphorylated K1250A CFTR. (A) Macroscopic current recording (top) from K1250A CFTR channels with simultaneously recorded temperature (bottom). Prephosphorylated channels were repeatedly opened by brief exposures to 10 mM MgATP, while bath temperature was toggled between 25°C (red box) and 15°C (blue box). Single exponentials (colored smooth lines) fitted to all current decay time courses at 25°C (red curves) and 15°C (blue curve) yielded time constants (τ) shown. (B) Eyring plot of normalized closing rates ($\hat{k}$) of K1250A CFTR channels upon ATP removal, fitted by a straight line to obtain $\Delta H^{\ddagger}$; closing rates, obtained as $1/\tau$ from single-exponential fits, as in A, were normalized to their average values in bracketing control segments at 25°C.

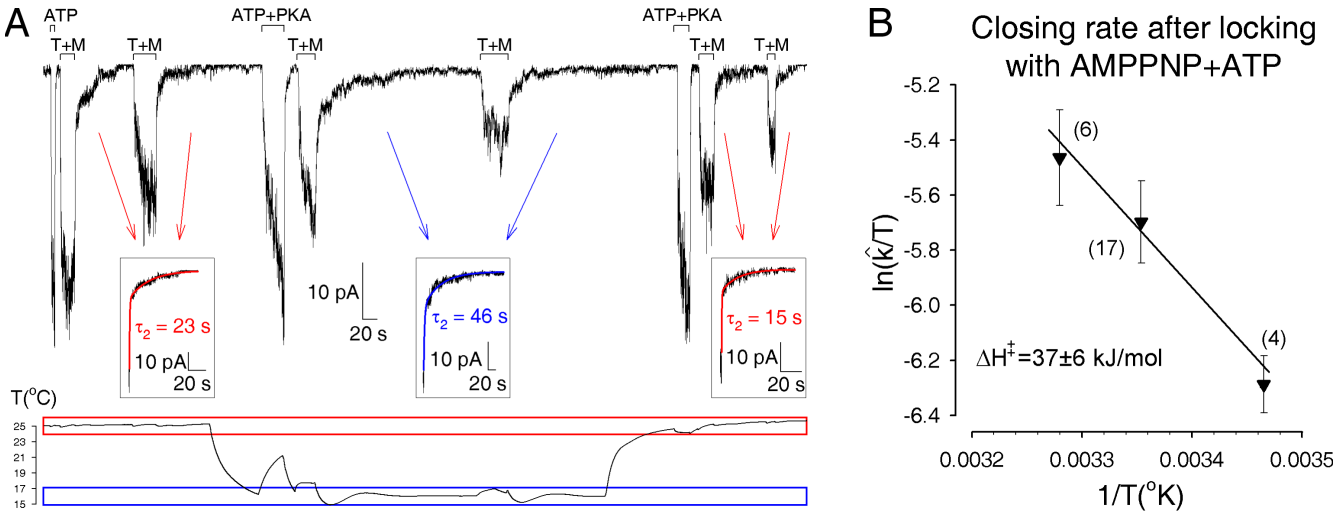

Figure 5. Temperature dependence of unlocking rate of WT CFTR channels locked open by ATP+AMPPNP. (A) Macroscopic current trace (top) from ~800 prephosphorylated WT CFTR channels, with simultaneously recorded temperature (bottom). Channels were repeatedly opened by brief exposures to 2 mM MgATP alone (bar, ATP) or with PKA (to reactivate dephosphorylated channels; bars, ATP+PKA), or to 0.1 mM MgATP+1 mM MgAMPPNP (bars, T+M), while bath temperature was toggled between 25°C (red box) and 16°C (blue box). Two consecutive decay time courses after removal of ATP+AMPPNP, in both test and bracketing segments, were summed to produce quasi-macroscopic time courses (insets) that were fit by double exponentials (colored smooth lines). (B) Unlocking rates of WT CFTR were obtained as the reciprocals of the slow time constants (as in A, insets, τ_2), and normalized to their average values in bracketing segments at 25°C; the resulting $\hat{k}$ were used to construct the Eyring plot shown.

(first vs. second current decay: Fig. 5 A and Fig. S4 B). This finding with partially phosphorylated CFTR channels contrasts with the ~90% of current that decays slowly, with ~30-s time constant, when locking is elicited by ATP+AMPPNP in the presence of PKA to maintain a high stoichiometry of phosphorylation (Csanády et al., 2000). We summed individual decay time courses after repeated exposures to ATP+AMPPNP to construct ensemble current decays, at 25°C and either 15°C (Fig. 5 A, insets) or 31°C (Fig. S4 B). From double-exponential fits to these decays (Fig. 5 A and Fig. S4 B, insets, smooth lines), the average fractional amplitude of the slow component at 25°C was 0.24 ± 0.02 (n = 17), and its average time constant was 10 ± 2 s (n = 17). From an Eyring plot of normalized unlocking rates (Fig. 5 B), the rough estimate of $\Delta H^{\ddagger}$ for unlocking from AMPPNP of partially phosphorylated WT CFTR was 37 ± 6 kJ/mol, similar to the value obtained above for closure of partially phosphorylated K1250R and K1250A channels opened by just ATP (Fig. 3 B and Fig. 4 B).

DISCUSSION

Both in the presence of PKA to sustain phosphorylation and shortly after its removal, allowing partial dephosphorylation, opening and closing rates of WT CFTR channels are strongly temperature dependent, though the temperature dependence of opening is steeper. Our results concur with those of one (Mathews et al., 1998b) of two earlier studies, but not with the other, which found practically no temperature dependence for channel closing rate (E_a = 10 kJ/mol; Aleksandrov and Riordan, 1998). The most likely reason for the discrepancy is that the latter study (Aleksandrov and Riordan, 1998) reported the temperature dependence of open times (which reflect the rate of entering the brief intraburst closed state—flickery closures; e.g., Haws et al., 1992), rather than that of open-burst durations (which reflect the rate of closing from bursts), as determined here (also in Mathews et al., 1998b). Because ATP and phosphorylation modulate the slow components of CFTR channel gating, i.e., the durations of interburst closures and of open bursts (e.g., Winter et al., 1994; Csanády et al., 2000; Vergani et al., 2003), but not the kinetics of the brief intraburst flickery closures (Vergani et al., 2003; Winter et al., 1994), analysis of the slow components, with time constants comparable to those of ATP hydrolysis by CFTR (Li et al., 1996), would seem more relevant for probing the mechanism of the ATP-driven CFTR gating cycle.

The fact that we obtained almost identical $\Delta H^{\ddagger}$ for closure of partially and of highly phosphorylated CFTR channels (69 ± 4 and 73 ± 5 kJ/mol; Fig. 1 C and Fig. 2) does not support the initial proposal that these reflect two qualitatively different closing mechanisms, with ATP hydrolysis at NBD2 limiting closure of only highly phosphorylated channels (Hwang et al., 1994; Gadsby and Nairn, 1999; Zeltwanger et al., 1999; Csanády et al., 2000). The fact that NBD2 catalytic site mutations dramatically prolong burst durations even after removal of PKA (Figs. 3 and 4), implies that ATP hydrolysis also limits the rate of closure of partially phosphorylated

channels. The same conclusion may be drawn from the observation that CFTR channels can be locked open by AMPPNP in the absence of PKA (Fig. 5 A; Fig. S4; compare Mathews et al., 1998a; Vergani et al., 2003), albeit with lower efficiency than when PKA is present (Hwang et al., 1994; Mathews et al., 1998a,b). So PKA seems to alter the rate, but not the chemical mechanism (hydrolysis of ATP), of the step that times channel closure. And, in energetic terms, the effect is not large. Thus, the shorter open burst durations that indicate a two- to threefold acceleration of channel closing after removal of PKA correspond to a change in $\Delta G^{\ddagger}$ for closure of only ~1kT (i.e., ~2 kJ/mol).

Because of its lower $\Delta G^{\ddagger}$ than for reversal of the opening reaction, this irreversible ATP hydrolysis step allows a WT channel to escape the open state by a pathway different from that by which it arrived (Gunderson and Kopito, 1994, 1995; Hwang et al., 1994; Carson et al., 1995; Zeltwanger et al., 1999; Dousmanis et al., 2002; Powe et al., 2002; Vergani et al., 2003, 2005). For this reason, the barrier heights for the opening and closing reactions cannot be compared to obtain thermodynamic state functions of the open state, relative to the closed state before opening. Instead, to estimate ΔH between those two states, $\Delta H^{\ddagger}$ for opening must be compared with $\Delta H^{\ddagger}$ for the closing reaction that represents reversal of opening, i.e., in the absence of ATP hydrolysis. We chose NBD2 catalytic site mutant K1250R as one model for nonhydrolytic closure because the mutation conserves charge in the anticipated catalytic interface, and, in P-glycoprotein, the corresponding K-to-R mutation essentially abolishes ATP hydrolysis (Lerner-Marmarosh et al., 1999). We selected the mutant K1250A as a second model for nonhydrolytic closure because it displays much slower closure than K1250R (e.g., Vergani et al., 2003, 2005) and because the K1250A mutation abolishes ATP hydrolysis by CFTR (Ramjeesingh et al., 1999). Finally, the closing rate of WT channels locked open by ATP+AMPPNP allowed an additional, independent, assessment. Although the rates of channel closure for these three nonhydrolytic models spanned a fivefold range (Fig. 3 A, Fig. 4 A, and Fig. 5 A), their temperature dependences, and thus $\Delta H^{\ddagger}$ values, were virtually identical (Fig. 3 B, Fig. 4 B, and Fig. 5 B).

Our $\Delta H^{\ddagger}$ estimates for opening, nonhydrolytic closure and normal (hydrolytic) closure allow us to construct a ΔH profile for the part of the CFTR channel (partially phosphorylated) gating cycle that includes a closed (interburst) state and subsequent open-burst state (Fig. 6 A, red line). The open and closed states in general cannot be compared because the system is not at thermodynamic equilibrium; after closure (to state C_ω; Fig. 6 A) the channel protein itself presumably returns to the closed conformation it assumed before opening (state C_α, Fig. 6 A), but the whole system has been changed by hydrolysis of ATP to ADP and inorganic phosphate (P_i). Nor can we compare thermodynamic state functions for the open state and the subsequent closed state, C_ω (Fig. 6 A, dotted lines), because that closing transition cannot be reversed (CFTR channels are not opened by ADP+P_i; Fig. S5) and so we cannot measure its $\Delta H^{\ddagger}$.

Uncertainty in the product of the prefactor A^* and transmission coefficient κ (see Materials and methods) means that we can derive only upper estimates for $\Delta G^{\ddagger}$ from the measured transition rates at 25°C (Fig. 6 A, blue line; the downward "smear" represents the direction of uncertainty). Moreover, κ might be different for a forward reaction and its reversal; e.g., $\kappa \approx 0.1$ and ≈ 0.3, respectively, for opening and closure of the diliganded acetylcholine receptor (Zhou et al., 2005). For this reason the errors in our estimates of $\Delta G^{\ddagger}$ for opening and for nonhydrolytic closure might also differ, so that the exact value of $\Delta G_{O\text{-}C_\alpha}$ is uncertain (symbolized by the break through the blue line; Fig. 6 A). The same considerations apply to the minimum estimates of $T\Delta S^{\ddagger}$ calculated from $\Delta H^{\ddagger}$ and $\Delta G^{\ddagger}_{max}$ (Fig. 6 A; broken green line with upward "smear" representing the direction of uncertainty).

Despite these limitations, we can safely draw several conclusions about the energetics of the CFTR gating cycle. First, from $\Delta H^{\ddagger} = 117$ kJ/mol versus $\Delta G^{\ddagger}_{max} = 76$ kJ/mol for opening, $\Delta S^{\ddagger}$ for opening must be substantial and positive ($T\Delta S^{\ddagger} \geq +41$ kJ/mol; Fig. 6 A, green line). Second, because $\Delta H^{\ddagger}$ is high (117 kJ/mol) for opening, but small for nonhydrolytic closure (e.g., 43 kJ/mol using K1250R as a model), $\Delta H_{O\text{-}C_\alpha}$ must be large (+74 kJ/mol; Fig. 6 A, red line). Third, in contrast, $\Delta G_{O\text{-}C_\alpha}$ is estimated to be rather small (e.g., −1 kJ/mol using K1250R as a model; Fig. 6 A, blue line), which in turn suggests that $\Delta S_{O\text{-}C_\alpha}$ is large ($T\Delta S_{O\text{-}C_\alpha} \approx$ 75 kJ/mol; Fig. 6 A, green line). The transmission coefficients for opening and nonhydrolytic closure would have to differ by a factor of 10^{13} to invalidate the latter conclusion, and that seems unlikely for κ values of a reaction and its reversal (compare Zhou et al., 2005). Also, independent evidence that $\Delta G_{O\text{-}C_\alpha} \approx 0$ is provided by the observation that steady-state $P_o \approx 0.5$ for the nonhydrolytic K1250R mutant, which is presumed to gate at thermodynamic equilibrium (Vergani et al., 2005). We may therefore safely conclude that the open state entropy is far higher than that of the preceding closed state. However, because our method tends to underestimate $T\Delta S^{\ddagger}$ (Fig. 6 A, upward green "smear"), we cannot exclude the possibility that during channel opening the entropy already reaches its full open-state value in the transition state, rather than increasing in two steps as presently indicated (Fig. 6 A, green line). Finally, our data provide no evidence that a large entropy change accompanies channel entry into the transition state for normal closure ($T\Delta S^{\ddagger} \geq -1$ kJ/mol; Fig. 6 A, green line, right), because $\Delta H^{\ddagger}$ (69 kJ/mol) is closely similar

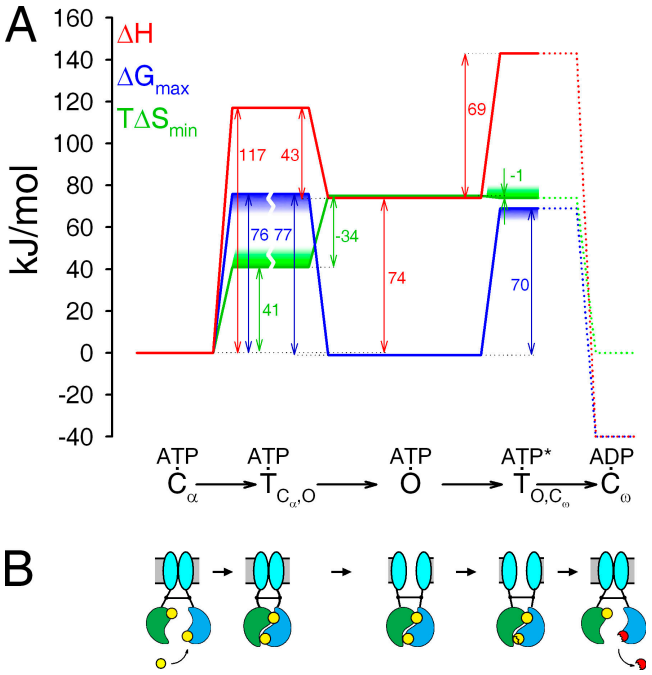

Figure 6. Energetic profile of gating of partially phosphorylated CFTR channels. (A) Profile of measured ΔH (red line), and computed ΔG_{max} (blue line), and $T\Delta S_{min}$ (green line) for a partially phosphorylated CFTR channel as it transits from an initial ATP-bound closed state (C_α) through a transition state ($T_{C_\alpha,O}$) to an open-burst state (O), and then through a different transition state (T_{O,C_ω}) to a final closed state (C_ω, with ADP at the binding site of the hydrolyzed ATP). Forward (left to right) $\Delta H^\ddagger$ values were obtained from slopes of Eyring plots for WT opening and closing rates (Fig. 1 C), $\Delta H^\ddagger$ for the reversal of opening reflects the slope of the Eyring plot for K1250R closing rate (Fig. 3B). Corresponding $\Delta G^\ddagger_{max}$ values were computed as $RT\ln(k_BT/(kh))$, by substituting the rates of WT opening ($0.3\ s^{-1}$) and closure ($3.9\ s^{-1}$), and of K1250R closure ($0.2\ s^{-1}$), for k. $T\Delta S^\ddagger_{min}$ was obtained as $\Delta H^\ddagger - \Delta G^\ddagger_{max}$. Downward blue and upward green "smear" on the ΔG_{max} and $T\Delta S_{min}$ lines, respectively, indicate the direction of possible error in those estimates; the breaks in those lines indicate uncertainty due to possible asymmetry in transmission coefficient κ (see text). Barrier heights from C_ω back to O could not be measured (dotted lines); ΔG for C_ω was tentatively drawn at ~−40 kJ/mol relative to C_α to represent hydrolysis of ATP at physiologically relevant concentrations of ATP, ADP, and P_i. (B) Cartoon illustrating mechanistic interpretation of the thermodynamic profile. Opening of the pore (cyan vertical ovals in gray horizontal membrane) is a consequence of formation of an NBD1(green)/NBD2(blue) tight dimer, with two ATP molecules (yellow circles) sandwiched in the interface. Channel closure normally follows hydrolysis of the ATP at the composite NBD2 catalytic site (lower site) to ADP (red) + P_i, which causes disruption of the dimer. The transition state for opening represents a strained channel molecule in which the NBD dimer is already formed but the transmembrane pore (cyan) is still closed. The transition state for normal closure represents the transition state for hydrolysis of the β-γ bond of the ATP (broken yellow circle).

to the upper estimate for $\Delta G^\ddagger$ (70 kJ/mol) for that step. Importantly, because that $T\Delta S^\ddagger$ is a lower estimate, our data exclude any significant decrease in entropy in the transition state for channel closure.

The paucity of ATPase measurements for CFTR mutants means that we cannot be certain that the charge-sparing mutation K1250R abolishes ATP hydrolysis in CFTR, even though the equivalent mutation in P-glycoprotein abolishes ATP hydrolysis (Lerner-Marmarosh et al., 1999). The charge-neutralizing mutation K1250A, on the other hand, does abrogate ATP hydrolysis in CFTR (Ramjeesingh et al., 1999) and yields an open burst state more stable than that of K1250R (Vergani et al., 2003, 2005). But using the closing rate of K1250A (instead of K1250R) channels as a model for nonhydrolytic closure, and hence for reversal of channel opening, yields barrier values for this step ($\Delta H^\ddagger$ = 39 kJ/mol and $\Delta G^\ddagger_{max}$ = 81 kJ/mol) that are only slightly different from those estimated using K1250R. Moreover, all the key features of the energy landscape (depicted in Fig. S6) remain unchanged. Even for the Walker B Glu mutant E1371Q CFTR channels, which display the most stable open-burst state observed for CFTR (closing time constant ~400 s; Vergani et al., 2005), corresponding to $\Delta G^\ddagger_{max}$ = 88 kJ/mol, if $\Delta H^\ddagger$ is assumed ~40 kJ/mol (its experimental determination would be a formidable task), the model predicts $\Delta G_{O\text{-}C_\alpha}$ = −12 kJ/mol, and again a similar overall energy profile.

Our thermodynamic measurements indicate that the transition state for opening of CFTR channels is characterized by an extremely large enthalpy, indicating molecular strain, together with a large increase in entropy. The latter supports the recent finding that conserved residues on opposing sides of the anticipated intramolecular NBD1–NBD2 dimer interface became energetically coupled in the transition state for CFTR channel opening, demonstrating that a tight NBD dimer had already then formed (Vergani et al., 2005). The entropy increase would reflect dehydration of the two interacting NBD surfaces and concomitant dispersal of the layer of bound (ordered) water molecules into the (disordered) bulk solution. The large enthalpy suggests that the transition state for opening is a strained CFTR protein conformation, with the tight NBD dimer already formed but the transmembrane pore still closed (Fig. 6 B); this is consistent with nucleotide-dependent channel opening being initiated at the NBDs. Pore opening should then partly relieve this strain, decreasing the enthalpy, as we found (Fig. 6 A). In simple terms, the energy of the power-stroke, provided by the extreme stability of the ATP-bound tight NBD1–NBD2 dimer, is used to load the gating spring (represented by curved connecting rods in Fig. 6 B), which then forces the gate to snap into its open conformation. This spreading conformational change, initiated by the gating machinery in the cytoplasm and propagated toward the transmembrane pore, echoes the mechanism recently proposed for opening of the nicotinic acetylcholine receptor, a true ligand-gated channel, after binding of its ligand acetylcholine some distance from the ion pore (Chakrapani et al., 2004).

But CFTR is not a true ligand-gated channel, because its open bursts appear to be normally terminated by ATP hydrolysis. This reaction invokes an enthalpy increase, unaccompanied by a change in entropy, caused by chemical bond strain without large conformational rearrangements, consistent with our observations on the transition state for closure. Because we can rule out an entropy decrease in this transition state (Fig. 6 A), we can conclude that the interacting NBD surfaces are still dehydrated and, hence, that the NBD1–NBD2 dimer is still intact; insofar as gating signals originate at the NBDs, we may further conclude that the pore is still open (Fig. 6 B). A simple interpretation is that the transition state for the step that rate limits CFTR channel closure represents the transition state for ATP hydrolysis (at the composite NBD2 catalytic site), and that the measured positive $\Delta H^{\ddagger}$ reflects strain in the ATP β-γ bond. This concurs both with the conclusion that ATP hydrolysis rate limits closure of WT CFTR channels (for example see Hwang et al., 1994; Gunderson and Kopito, 1994, 1995; Carson et al., 1995; Zeltwanger et al., 1999; Dousmanis et al., 2002; Powe et al., 2002; Vergani et al., 2003, 2005), and with $\Delta H^{\ddagger}$ values measured for turnover of other ATP- and GTPases (Tu et al., 1988; Mejillano et al., 1996). Upon cleavage of the γ-phosphate from the nucleotide, the enthalpy of the strained β-γ bond is used to diminish the entropy of the open state, as the channel pore adopts its closed conformation and an ordered layer of water molecules covers the NBD surfaces exposed by disruption of the tight dimer interface.

We thank Dr. Paola Vergani for helpful discussion and Dóra Takács for oocyte isolation and injection.

This work was supported by NIH DK51767 and NIH Fogarty International Center grant R03-TW05761.

Christopher Miller served as editor.

Submitted: 13 April 2006
Accepted: 20 September 2006

REFERENCES

Aleksandrov, A.A., and J.R. Riordan. 1998. Regulation of CFTR ion channel gating by MgATP. *FEBS Lett.* 431:97–101.

Aleksandrov, A.A., X. Chang, L. Aleksandrov, and J.R. Riordan. 2000. The non-hydrolytic pathway of cystic fibrosis transmembrane conductance regulator ion channel gating. *J. Physiol.* 528:259–265.

Aleksandrov, A.A., L. Aleksandrov, and J.R. Riordan. 2002. Nucleoside triphosphate pentose ring impact on CFTR gating and hydrolysis. *FEBS Lett.* 518:183–188.

Anderson, M.P., H.A. Berger, D.P. Rich, R.J. Gregory, A.E. Smith, and M.J. Welsh. 1991. Nucleoside triphosphates are required to open the CFTR chloride channel. *Cell.* 67:775–784.

Basso, C., P. Vergani, A.C. Nairn, and D.C. Gadsby. 2003. Prolonged nonhydrolytic interaction of nucleotide with CFTR's NH_2-terminal nucleotide binding domain and its role in channel gating. *J. Gen. Physiol.* 122:333–348.

Baukrowitz, T., T.C. Hwang, A.C. Nairn, and D.C. Gadsby. 1994. Coupling of CFTR Cl^- channel gating to an ATP hydrolysis cycle. *Neuron.* 12:473–482.

Bompadre, S.G., J.H. Cho, X. Wang, X. Zou, Y. Sohma, M. Li, and T.C. Hwang. 2005. CFTR gating II: effects of nucleotide binding on the stability of open states. *J. Gen. Physiol.* 125:377–394.

Cai, Z., T.S. Scott-Ward, and D.N. Sheppard. 2003. Voltage-dependent gating of the cystic fibrosis transmembrane conductance regulator Cl^- channel. *J. Gen. Physiol.* 122:605–620.

Carson, M.R., S.M. Travis, M.C. Winter, D.N. Sheppard, and M.J. Welsh. 1994. Phosphate stimulates CFTR Cl^- channels. *Biophys. J.* 67:1867–1875.

Carson, M.R., S.M. Travis, and M.J. Welsh. 1995. The two nucleotide-binding domains of cystic fibrosis transmembrane conductance regulator (CFTR) have distinct functions in controlling channel activity. *J. Biol. Chem.* 270:1711–1717.

Chakrapani, S., and A. Auerbach. 2005. A speed limit for conformational change of an allosteric membrane protein. *Proc. Natl. Acad. Sci. USA.* 102:87–92.

Chakrapani, S., T.D. Bailey, and A. Auerbach. 2004. Gating dynamics of the acetylcholine receptor extracellular domain. *J. Gen. Physiol.* 123:341–356.

Chan, K.W., L. Csanády, D. Seto-Young, A.C. Nairn, and D.C. Gadsby. 2000. Severed molecules functionally define the boundaries of the cystic fibrosis transmembrane conductance regulator's NH(2)-terminal nucleotide binding domain. *J. Gen. Physiol.* 116:163–180.

Chang, X.B., J.A. Tabcharani, Y.X. Hou, T.J. Jensen, N. Kartner, N. Alon, J.W. Hanrahan, and J.R. Riordan. 1993. Protein kinase A (PKA) still activates CFTR chloride channel after mutagenesis of all 10 PKA consensus phosphorylation sites. *J. Biol. Chem.* 268:11304–11311.

Cheng, S.H., D.P. Rich, J. Marshall, R.J. Gregory, M.J. Welsh, and A.E. Smith. 1991. Phosphorylation of the R domain by cAMP-dependent protein kinase regulates the CFTR chloride channel. *Cell.* 66:1027–1036.

Colquhoun, D., and F.J. Sigworth. 1995. Fitting and statistical analysis of single-channel records. *In* Single Channel Recording. B. Sakmann and E. Neher, editors. Plenum Press, New York. 483–587.

Csanády, L. 2000a. Rapid kinetic analysis of multichannel records by a simultaneous fit to all dwell-time histograms. *Biophys. J.* 78:785–799.

Csanády, L. 2000b. Structure-function studies on human epithelial cystic fibrosis chloride channels expressed in *Xenopus laevis* oocytes. Ph.D. thesis. The Rockefeller University, New York. 212 pp.

Csanády, L., K.W. Chan, D. Seto-Young, D.C. Kopsco, A.C. Nairn, and D.C. Gadsby. 2000. Severed channels probe regulation of gating of cystic fibrosis transmembrane conductance regulator by its cytoplasmic domains. *J. Gen. Physiol.* 116:477–500.

Csanády, L., D. Seto-Young, K.W. Chan, C. Cenciarelli, B.B. Angel, J. Qin, D.T. McLachlin, A.N. Krutchinsky, B.T. Chait, A.C. Nairn, and D.C. Gadsby. 2005. Preferential phosphorylation of R-domain serine 768 dampens activation of CFTR channels by PKA. *J. Gen. Physiol.* 125:171–186.

Dousmanis, A.G., A.C. Nairn, and D.C. Gadsby. 2002. Distinct Mg(2+)-dependent steps rate limit opening and closing of a single CFTR Cl^- channel. *J. Gen. Physiol.* 119:545–559.

Fersht, A. 1999. Structure and Mechanism in Protein Science. W.H. Freeman and Co., New York. 631 pp.

Frisch, C., A.R. Fersht, and G. Schreiber. 2001. Experimental assignment of the structure of the transition state for the association of barnase and barstar. *J. Mol. Biol.* 308:69–77.

Gadsby, D.C., and A.C. Nairn. 1999. Control of CFTR channel gating by phosphorylation and nucleotide hydrolysis. *Physiol. Rev.* 79: S77–S107.

Gadsby, D.C., P. Vergani, and L. Csanády. 2006. The ABC protein turned chloride channel whose failure causes cystic fibrosis. *Nature.* 440:477–483.

Gunderson, K.L., and R.R. Kopito. 1994. Effects of pyrophosphate and nucleotide analogs suggest a role for ATP hydrolysis in cystic

fibrosis transmembrane regulator channel gating. *J. Biol. Chem.* 269:19349–19353.

Gunderson, K.L., and R.R. Kopito. 1995. Conformational states of CFTR associated with channel gating: the role ATP binding and hydrolysis. *Cell.* 82:231–239.

Hagen, S.J., J. Hofrichter, A. Szabo, and W.A. Eaton. 1996. Diffusion-limited contact formation in unfolded cytochrome c: estimating the maximum rate of protein folding. *Proc. Natl. Acad. Sci. USA.* 93:11615–11617.

Hamill, O.P., A. Marty, E. Neher, B. Sakmann, and F.J. Sigworth. 1981. Improved patch-clamp techniques for high-resolution current recording from cells and cell-free membrane patches. *Pflugers Arch.* 391:85–100.

Haws, C., M.E. Krouse, Y. Xia, D.C. Gruenert, and J.J. Wine. 1992. CFTR channels in immortalized human airway cells. *Am. J. Physiol.* 263:L692–L707.

Hopfner, K.P., A. Karcher, D.S. Shin, L. Craig, L.M. Arthur, J.P. Carney, and J.A. Tainer. 2000. Structural biology of Rad50 ATPase: ATP-driven conformational control in DNA double-strand break repair and the ABC-ATPase superfamily. *Cell.* 101:789–800.

Hwang, T.C., G. Nagel, A.C. Nairn, and D.C. Gadsby. 1994. Regulation of the gating of cystic fibrosis transmembrane conductance regulator C1 channels by phosphorylation and ATP hydrolysis. *Proc. Natl. Acad. Sci. USA.* 91:4698–4702.

Kaczmarek, L.K., K.R. Jennings, F. Strumwasser, A.C. Nairn, U. Walter, F.D. Wilson, and P. Greengard. 1980. Microinjection of catalytic subunit of cyclic AMP-dependent protein kinase enhances calcium action potentials of bag cell neurons in cell culture. *Proc. Natl. Acad. Sci. USA.* 77:7487–7491.

Lerner-Marmarosh, N., K. Gimi, I.L. Urbatsch, P. Gros, and A.E. Senior. 1999. Large scale purification of detergent-soluble P-glycoprotein from *Pichia pastoris* cells and characterization of nucleotide binding properties of wild-type, Walker A, and Walker B mutant proteins. *J. Biol. Chem.* 274:34711–34718.

Li, C., M. Ramjeesingh, W. Wang, E. Garami, M. Hewryk, D. Lee, J.M. Rommens, K. Galley, and C.E. Bear. 1996. ATPase activity of the cystic fibrosis transmembrane conductance regulator. *J. Biol. Chem.* 271:28463–28468.

Mathews, C.J., J.A. Tabcharani, X.B. Chang, T.J. Jensen, J.R. Riordan, and J.W. Hanrahan. 1998a. Dibasic protein kinase A sites regulate bursting rate and nucleotide sensitivity of the cystic fibrosis transmembrane conductance regulator chloride channel. *J. Physiol.* 508(Pt. 2):365–377.

Mathews, C.J., J.A. Tabcharani, and J.W. Hanrahan. 1998b. The CFTR chloride channel: nucleotide interactions and temperature-dependent gating. *J. Membr. Biol.* 163:55–66.

Mejillano, M.R., B.D. Shivanna, and R.H. Himes. 1996. Studies on the nocodazole-induced GTPase activity of tubulin. *Arch. Biochem. Biophys.* 336:130–138.

Nagel, G., T.C. Hwang, K.L. Nastiuk, A.C. Nairn, and D.C. Gadsby. 1992. The protein kinase A-regulated cardiac Cl^- channel resembles the cystic fibrosis transmembrane conductance regulator. *Nature.* 360:81–84.

Powe, A.C., Jr., L. Al Nakkash, M. Li, and T.C. Hwang. 2002. Mutation of Walker-A lysine 464 in cystic fibrosis transmembrane conductance regulator reveals functional interaction between its nucleotide-binding domains. *J. Physiol.* 539:333–346.

Qin, F., A. Auerbach, and F. Sachs. 1996. Estimating single-channel kinetic parameters from idealized patch-clamp data containing missed events. *Biophys. J.* 70:264–280.

Ramjeesingh, M., C. Li, E. Garami, L.J. Huan, K. Galley, Y. Wang, and C.E. Bear. 1999. Walker mutations reveal loose relationship between catalytic and channel-gating activities of purified CFTR (cystic fibrosis transmembrane conductance regulator). *Biochemistry.* 38:1463–1468.

Riordan, J.R., J.M. Rommens, B. Kerem, N. Alon, R. Rozmahel, Z. Grzelczak, J. Zielenski, S. Lok, N. Plavsic, J.L. Chou, et al. 1989. Identification of the cystic fibrosis gene: cloning and characterization of complementary DNA. *Science.* 245:1066–1073.

Schweins, T., and A. Warshel. 1996. Mechanistic analysis of the observed linear free energy relationships in p21ras and related systems. *Biochemistry.* 35:14232–14243.

Smith, P.C., N. Karpowich, L. Millen, J.E. Moody, J. Rosen, P.J. Thomas, and J.F. Hunt. 2002. ATP binding to the motor domain from an ABC transporter drives formation of a nucleotide sandwich dimer. *Mol. Cell.* 10:139–149.

Tabcharani, J.A., X.B. Chang, J.R. Riordan, and J.W. Hanrahan. 1991. Phosphorylation-regulated Cl^- channel in CHO cells stably expressing the cystic fibrosis gene. *Nature.* 352:628–631.

Tu, S.I., J.N. Brouillette, G. Nagahashi, D. Brauer, and E. Nungesser. 1988. Temperature dependence and mercury inhibition of tonoplast-type H^+-ATPase. *Arch. Biochem. Biophys.* 266:289–297.

Vergani, P., A.C. Nairn, and D.C. Gadsby. 2003. On the mechanism of MgATP-dependent gating of CFTR Cl^- channels. *J. Gen. Physiol.* 121:17–36.

Vergani, P., S.W. Lockless, A.C. Nairn, and D.C. Gadsby. 2005. CFTR channel opening by ATP-driven tight dimerization of its nucleotide-binding domains. *Nature.* 433:876–880.

Walker, J.E., M. Saraste, M.J. Runswick, and N.J. Gay. 1982. Distantly related sequences in the α- and β-subunits of ATP synthase, myosin, kinases and other ATP-requiring enzymes and a common nucleotide binding fold. *EMBO J.* 1:945–951.

Winter, M.C., D.N. Sheppard, M.R. Carson, and M.J. Welsh. 1994. Effect of ATP concentration on CFTR Cl^- channels: a kinetic analysis of channel regulation. *Biophys. J.* 66:1398–1403.

Zeltwanger, S., F. Wang, G.T. Wang, K.D. Gillis, and T.C. Hwang. 1999. Gating of cystic fibrosis transmembrane conductance regulator chloride channels by adenosine triphosphate hydrolysis. Quantitative analysis of a cyclic gating scheme. *J. Gen. Physiol.* 113:541–554.

Zhou, Y., J.E. Pearson, and A. Auerbach. 2005. Phi-value analysis of a linear, sequential reaction mechanism: theory and application to ion channel gating. *Biophys. J.* 89:3680–3685.